Deaggregation of Nanodiamond Powders Using Salt- and Sugar-Assisted Milling

Amanda Pentecost,[†] Shruti Gour,[†,‡] Vadym Mochalin,[†] Isabel Knoke,[†,§] and Yury Gogotsi*[,†]

Department of Materials Science and Engineering, A.J. Drexel Nanotechnology Institute and Department of Biomedical Engineering, Drexel University, Philadelphia, Pennsylvania 19104, United States

ABSTRACT Diamond particles of 5−10 nm in size can be produced in large quantities by denonating oxygen-lean explosives in a closed chamber. They have numerous useful properties and are used in applications ranging from lubricants to drug delivery. Aggregation of diamond nanoparticles is limiting wider use of this important carbon nanomaterial because most applications require single separated particles. We demonstrate that dry media assisted attrition milling is a simple, inexpensive, and efficient alternative to the current ways of deaggregating of nanodiamond. This technique uses water-soluble nontoxic and noncontaminating crystalline compounds, such as sodium chloride or sucrose. When milling is complete, the media can be easily removed from the product by water rinsing, which provides an advantage when compared to milling with ceramic microbeads. Using the dry media assisted milling with subsequent pH adjustment, it is possible to produce stable aqueous nanodiamond colloidal solutions with particles <10 nm in diameter, which corresponds to 1−2 primary nanodiamond particles. The study of milling kinetics and the characterization of the produced nanodiamond colloids led us to conclude that aggregates of less than 200 nm in diameter, observed at the tail of the pore size distribution of milled nanodiamond, are loosely bonded and rather dynamic in nature. Color change observed in ND colloids upon shifting their pH toward the basic end allowed us to demonstrate that the coloration comes from the light interaction with colloidal particles and not from an increase in nondiamond carbon content.

KEYWORDS: nanodiamond • ultradispersed diamond • deaggregation • nanodiamond dispersions • nanodiamond colloids • attrition milling

1. INTRODUCTION

While nanotubes, fullerenes, and graphene form the basis of academic and commercial carbon research, other nanocarbons, such as nanodiamond powder (ND) produced by detonation synthesis (a process discovered in the former USSR in the early 1960s and reproduced in the U.S.A. in the late 1980s 1–5), remain less understood. Currently, large-scale commercial production of ND is established in Russia, China, Japan, and several European countries. The rise of interest in nanodiamond is the result of its many unique properties, including superior hardness and Young's modulus, high electrical resistivity, attractive optical characteristics, and excellent chemical stability and biocompatibility, all of which it inherits from bulk diamond and delivers on the nanometer scale, in the form of ∼5 nm primary particles with large accessible surface bearing a variety of reactive functional groups (3).

Essentially all existing and future applications of ND critically depend on the small particle size (6). However, as compared to other nanomaterials, the detonation nanodiamonds have an unusually strong tendency to aggregate, which makes the primary ND particles very difficult to isolate and keep separated (7). The nature of these ND aggregates is still not clearly understood. It is hypothesized that the extreme conditions in the detonation wave result in dangling bonds on the surface of ND particles that, in later stages, when temperature and pressure drop, react and either form strong covalent interparticle bonds, graphitic shells (which may engulf several ND primary particles and hold them together in a strongly bonded aggregate) or surface functional groups, which can also cause aggregation via hydrogen bond formation or dipole−dipole and weak van der Waals interactions between the functional groups on adjacent ND particles. A. Krueger et al. (7) have proposed a hierarchical model of the ND aggregates, subdividing them into agglomerates (20−30 μm), intermediate aggregates (2−3 μm), and core aggregates (100−200 nm). While agglomerates and intermediate aggregates can be disintegrated by mild or powerful sonication, the core aggregates, according to ref 7, are very strong and cannot be broken up by any conventional mechanical, ultrasound, or surfactant-assisted techniques. For the core ND aggregates, a model was proposed in which primary ND particles are embedded into an amorphous and graphitic carbon matrix holding them together. However, the very existence of core aggregates and the actual role of strong interparticle bonding in ND aggregation still remains an open question. For example, A. Barnard and E. Osawa have recently put forward an alternative model of ND aggregates (6, 8), in which the primary role is taken off the covalent or van der Waals interparticle interactions and is assigned to the electrostatic forces due to spontaneous

* To whom correspondence should be addressed. E-mail: gogotsi@drexel.edu.
Received for review August 11, 2010 and accepted October 13, 2010

† Department of Materials Science and Engineering and A.J. Drexel Nanotechnology Institute.

‡ Department of Biomedical Engineering.

§ Current affiliation: Center for Nanoanalysis and Electron Microscopy (CENEM), Department of Material Science and Engineering WW 7, University of Erlangen-Nürnberg, 91058 Erlangen, Germany.

DOI: 10.1021/am100720n

charge separation occurring on different faces of polyhedral primary ND particles. This model is based on results of the density functional theory model (9) and has no related experimental proofs so far.

With ongoing research and different points of view on the nature of the ND aggregates, the ultimate goal, however, still remains unchanged: to produce the smallest possible ND particles and keep them separated. As of now, several techniques are known for the disintegration of ND aggregates. Some of them are closely related to ND purification. For example, amorphous carbon and graphitic shells holding particles together, as well as some interparticle covalent bonds, can be eliminated by liquid (see ref 10 for references) or gas phase (10–12) oxidation. As a result of oxidation, the size of ND aggregates decreases. Although separate single ND particles were found in the transmission electron microscopy (TEM) observations of powders oxidized in air (11), large (>100 nm in diameter) agglomerates were formed when the oxidized ND was dispersed in aqueous media. Seemingly paradoxical, graphitization has also been used in an attempt to disintegrate the ND aggregates. In the graphitization−oxidation process (12), a thin graphitic layer is deliberately formed on the surface of ND and subsequently removed by air or liquid oxidation exploiting known oxidation chemistry of curved graphitic carbon. The product was sonicated in water, and the authors report (12) that more than 50% of particles in the aqueous suspension have a diameter of less than 50 nm. At the same time, the formation of ND aggregates of 1−2 μm, that is, larger than the size of initial aggregates, was observed. The latter was explained by interparticle covalent bond formation favored by oxidation (12, 13). However, in our opinion, incomplete removal of the graphitic layer formed at the graphitization step may also contribute to the observed enlargement of the ND aggregates. Moreover, the formation of an additional amount of sp^2 carbon in ND is often undesirable. Therefore, simple oxidation of ND in air (11) with subsequent aqueous hydrochloric acid treatment to remove traces of metals and convert surface anhydrides into acids could produce similar or better results.

Extreme deaggregation techniques, such as high dynamic pressure pulse, created by an electromagnetic gun were used (14), but their efficiency is not known since details regarding the particle size were not provided. It is obvious that being of interest for research purposes, these methods are unlikely to be implemented in mass production where less complicated and less expensive techniques are required.

Traditional mechanical means, such as wet milling of ND with SiO_2 microbeads in aqueous environment, did not produce primary particles. Only being combined with subsequent high power sonication for up to 1 h did it result in a stable 5 nm ND suspension (7). The wet milling technique was later modified (15, 16): critical parts of the mill, such as a vessel and an agitator, were made of zirconia instead of steel, and SiO_2 microbeads were replaced by ZrO_2 microbeads to minimize wearing and leave less contaminations in ND. Another technique has also been introduced in ref 15 called bead-assisted sonic disintegration (BASD), which includes the high power sonication of a ND slurry with ZrO_2 beads. BASD resulted in a remarkable decrease in the particle size: ND particles smaller than 10 nm were produced within 2 h of sonication. However, ZrO_2 contamination left in ND after either milling or BASD is very difficult to remove because zirconia is highly resistant to most acids/bases, affecting biomedical and other applications of the ND.

There were attempts to disintegrate ND aggregates using mechanochemical treatment, that is, milling in the presence of chemicals such as surfactants and electrolytes (e.g., sodium oleate) (17, 18). Mechanical action was applied in the form of grinding or sonication in the presence of sodium oleate and resulted in a reduction of the aggregate size of thus treated ND in water from 2 μm down to 40−60 nm (18). However, no particles smaller than 20 nm were observed.

Consequently, literature shows that, of the well-documented techniques, only ZrO_2 microbead-assisted wet milling and BASD are currently capable of breaking the core ND aggregates and producing stable suspensions consisting of primary ND particles (6). However, contamination of ND with difficult-to-remove zirconia, the high cost of zirconia microbeads, and ND amorphization (or even graphitization) in the course of milling are major drawbacks of the microbeads-assisted milling.

Recently, we have demonstrated that sodium chloride is efficient as a medium in dry milling of a cholesterol-reducing drug, fenofibrate (19). A particular advantage of this innovative approach is that when the milling is complete, sodium chloride could be easily washed out with water leaving no contaminations in the product.

In this paper, we extend the dry salt assisted milling technique and demonstrate its feasibility as a novel simple and cost-effective approach to disintegrate ND aggregates. We also show that substances other than NaCl, such as sugar (i.e., nontoxic, inexpensive, sufficiently hard, and easily removable by water rinsing), can be used for this purpose, thus opening the way to mass-production of deagglomerated ND powders and colloids.

2. MATERIALS AND METHODS

Nanodiamond powder (UD90 grade) was obtained from Nanoblox, Inc., U.S.A., and used without subsequent purification. Sodium chloride and sucrose were purchased from Sigma-Aldrich, U.S.A., with particle sizes of 80 and 72 mesh respectively.

A temperature controlled lab attrition mill with a 110 cm^3 milling chamber and stainless steel grinding balls, 0.635 cm (1/4 in.) in diameter, was designed and manufactured by Union Process, Inc., U.S.A. The vessel was cooled to 0 °C and maintained at this temperature for the course of milling to minimize thermal damage of the sample by heat generated by friction and impact. The mill was loaded with a charge consisting of nanodiamond powder, dry milling media (sodium chloride or sucrose), and 538.6 g (19 oz) grinding steel balls (Figure 1a). The charge was milled with varying time at 500 rpm and 1:7 nanodiamond:milling media ratio.

The milled nanodiamond was repeatedly rinsed with DI water in a 500 mL beaker until negative test with 0.1 N silver nitrate (when NaCl was used as a milling media). In the case of sugar, rinsing was performed 6 times to ensure that the sugar had been

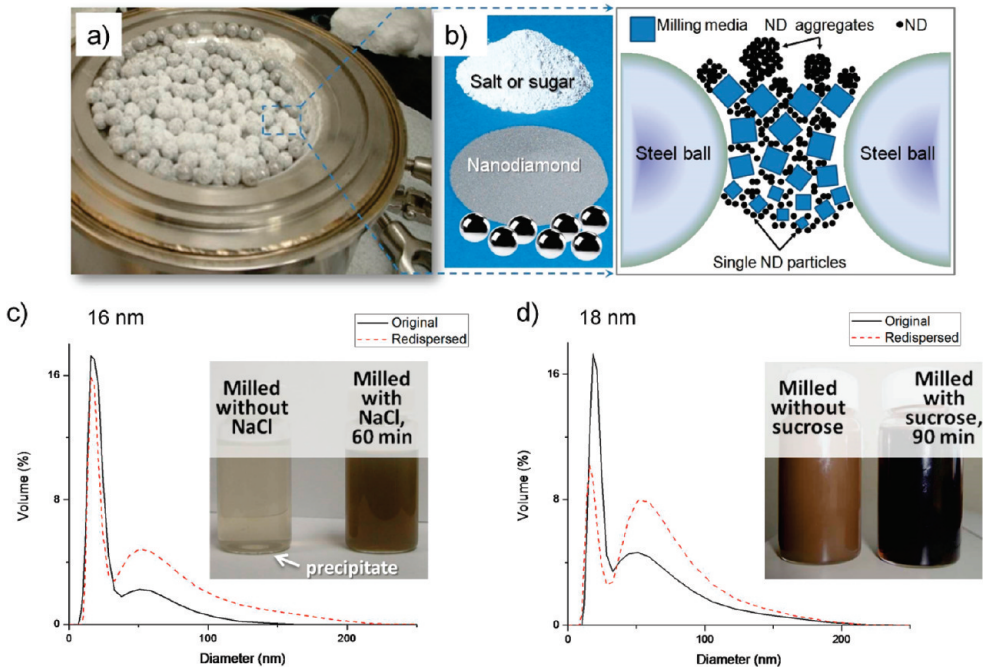

FIGURE 1. Photograph of the milling chamber filled with stainless steel balls, nanodiamond, and salt (a) and a schematic of the media assisted dry milling deaggregation process (b). Particle size distribution (pH adjusted to ~11) and photographs of aqueous nanodiamond dispersions milled with NaCl (c) and sucrose (d). Original corresponds to milled material after water rinsing and pH adjustment to ~11. Redispersed corresponds to milled material after water rinsing, pH adjustment to ~11, drying, re-dispersing in water and re-adjusting pH to ~11.

completely removed. After the last rinsing, ND still partially precipitated from the suspension because its concentration was too high to maintain a stable system. Once the equilibrium was established, the part that remained in the suspension was taken and used for subsequent tests.

Malvern Zetasizer Nano ZS with an MPT-2 autotitrator was used for particle size and zeta-potential vs pH measurements.

TEM analysis was carried out on a JEOL JEM-2100 microscope with an operating voltage of 200 kV. Samples for TEM were produced by dipping the lacey carbon coated Cu grid into the aqueous ND colloidal solution and letting it dry in air. The TEM used in this study is equipped with a high tilt sample holder allowing tilt angles up to ±60°. Serial EM software was used to record the tilt series and IMOD software was used for reconstruction of tomograms.

3. RESULTS

It is known that the size of the milling bodies needs to be on the order of the size of the milled material, so that the effective contact area and the efficiency of milling are maximized (20). Traditional milling using macro-sized balls is not effective when the size of the milled material is in the submicrometer domain. In order to mill micro- and nanopowders, micrometer-sized media are required. In particular, expensive silica and zirconia microbeads were used in prior studies on disintegration of ND aggregates (7, 15, 16). An alternative novel approach is to reduce the size of the milling media by milling them along with the particles of milled material so that both are kept on the same size scale during the entire milling process (19). This allows one to keep the milling efficiency high by maintaining the balance between the sizes of the milled particles and the milling bodies automatically in situ as schematically shown in Figure 1b. Crystalline powders, such as sodium chloride, sucrose, and other similar substances, are hard enough to mill many soft organics, while they are comminuted themselves by larger steel balls that supply mechanical energy to the system. The hardness of ND primary particles is very high; therefore, we do not expect the milling media to reduce the size of ND primary particles. However, we do expect that the milling media will assist in breaking the ND aggregates to the state of primary particles. Additionally, the small particles of the milling media produced *in situ*, are expected to surround and isolate the particles of ND, thus preventing their reagglomeration. In our prior study on milling fenofibrate with NaCl (19), we have shown that the milling efficiency depends on rotation speed, salt to fenofibrate ratio, and time. We have found that, for our mill, the milling efficiency is lower for the speeds higher than 500 rpm. This is probably because of a high correlation in motion of balls that occurs at higher speeds when the balls, milling media, and the milled material slide over the milling chamber walls as a single body. This significantly reduces the number of collisions between the milling balls and hence, the milling efficiency. When the fenofibrate to salt ratio decreased, the milling efficiency increased, although setting this parameter too low reduces the yield of the product and is not practically reasonable at values less than 1:7. Therefore, in our current study, we fixed rotation speed at 500 rpm and ND to salt ratio at 1:7, while varying time of milling. Since we use a steel milling chamber and steel milling balls in this study, we are aware of possible contamination of nanodiamond with iron. Fortunately, this contamination can easily be removed via subsequent acid treatment of ND with aqueous HCl.

Milling kinetics data is presented in Figure 2a, b. In the beginning, the particle size distribution (PSD) of as-received

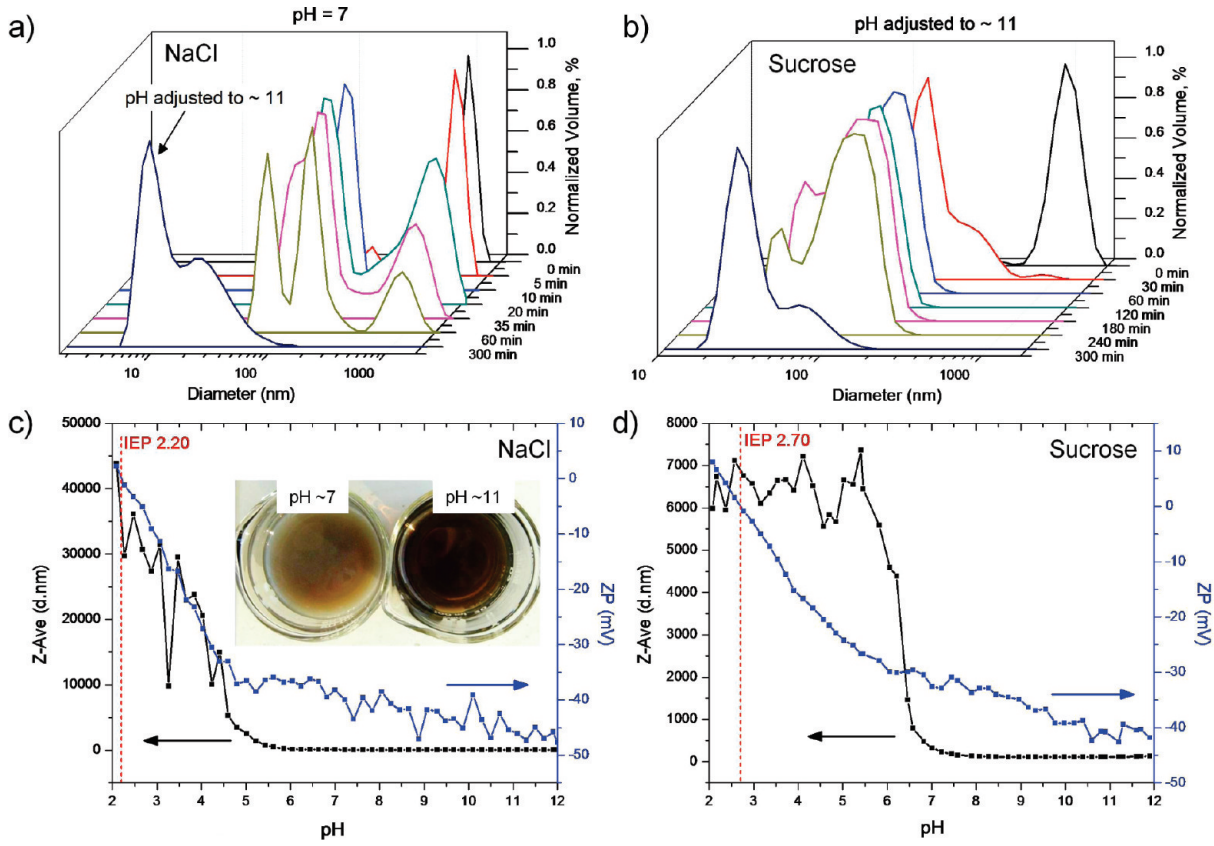

FIGURE 2. Particle size distribution of milled nanodiamond aqueous dispersions as a function of milling time; with NaCl (a) and sucrose (b). Particle size and zeta potential of aqueous milled nanodiamond (milling time 5 h) as a function of pH are shown in (c) for NaCl and (d) for sucrose. Inset in (c) shows photographs of NaCl milled ND (90 min milling time) colloidal solutions before and after the addition of 0.5 mL of 0.1 M NaOH to adjust pH at ~11.

ND dispersed in water is centered at about 1000 nm. After only 5 min of salt assisted milling, smaller particles (peak at 150−200 nm) appear in the PSD, while the peak at 1000 nm decreases in intensity (Figure 2a). Longer milling times result in a further decrease in the number and size of larger aggregates; meanwhile, the smaller particles increase in number and decrease in size. Thus, what was observed in milling is a complex behavior where not only the size, but also the proportion of particles of different size is changing continuously over time. The kinetics is characterized by the change in polydispersity of ND, the appearance of shoulder peaks in the PSD, the production of intermediate fractions of particles (an intermediate third peak seen at 35 and 60 min in Figure 2a), and the subsequent transformation and merger of the fractions with each other. After 5 h of milling and adjusting pH to ~11, the majority of particles is small (~10 nm in diameter) with a small tail in the distribution extending up to ~100 nm (Figure 2a).

TEM studies confirm the deaggregation of nanodiamond by milling (Figure 3). High-resolution TEM micrographs of NaCl milled ND sample show separate ND particles lying close to each other on an amorphous carbon film support (Figure 3a, b). This clustering of ND particles is due to the surface tension of water upon drying and is quite different in appearance from the aggregates observed in as-received, nonmilled material. The difference is even more emphasized in the 3-D reconstructed TEM electron tomograms shown in Figure 3c, d. While the as-received nanodiamond typically forms large, dense, 3-D aggregates of hundreds of nanometers in size, milled material shows only small 15−20 nm nanodiamond particles uniformly seeded on the edges of the film after drying (Figure 3d).

It is known that as-received ND has a large number of carboxylic groups attached to its surface (11, 21) as a result of oxidative purification used by manufacturers. Therefore, one could expect that in a basic environment, which favors dissociation of the carboxyl groups (eq 1), an increased negative surface charge on ND particles due to COO^- should result in a stronger repulsion of the individual particles and improved colloid stability.

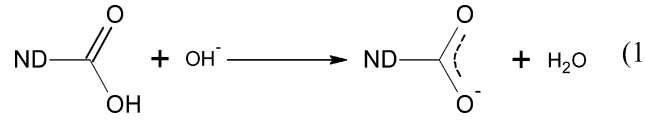

(1)

To verify this assumption and find an optimal pH for dispersions, we studied size and zeta potential of the particles as functions of pH (Figure 2c, d). Measured zeta potential is negative and decreasing from −(30−35) mV at pH 7 to −(40−45) mV at pH 12. As a result, the particle size is minimal in this pH range. Based on the titration data, we adjusted pH of aqueous suspensions of milled ND at 11.4 by adding 5−7 drops of 0.1 M NaOH to 10 mL of the ND suspension. pH adjustment was adopted as a routine procedure for all sucrose milled samples (Figure 2b), while for

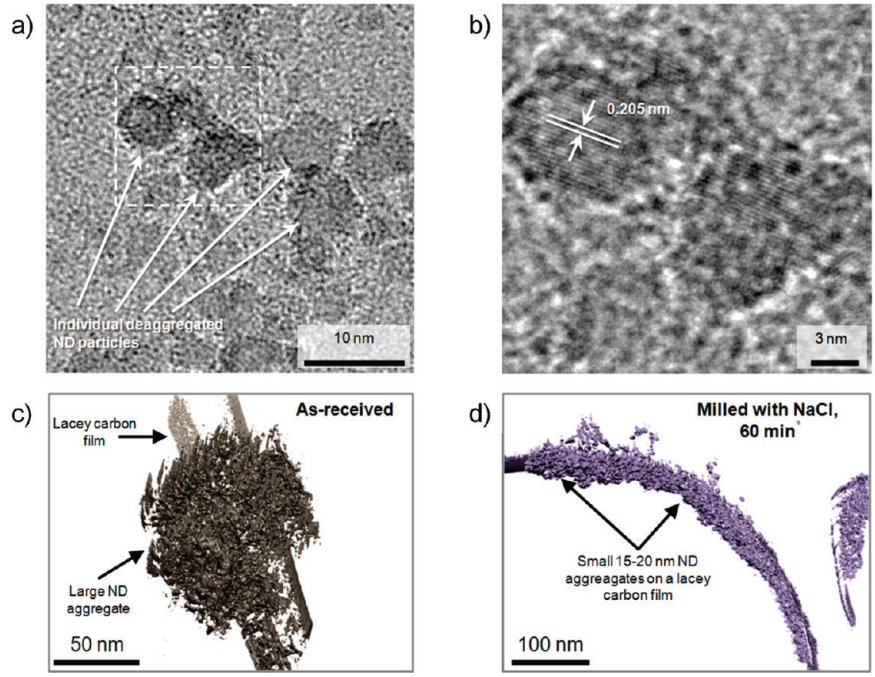

FIGURE 3. (a) Low-resolution and (b) high resolution TEM images of nanodiamond milled with NaCl for 60 min. Panel b is a close up of the boxed region marked in panel a; 3-D reconstruction of electron tomograms of as-received (c) and milled nanodiamond (d) on lacey carbon support.

salt milled samples it was used only in selected cases. Combined with milling, pH adjustment leads to a substantial reduction in the amount of larger aggregates (Figure 2b) as compared to nonadjusted suspensions (Figure 2a). Therefore, the aggregates with diameters larger than 100 nm observed in milling kinetics studies without subsequent pH adjustment (Figure 2a) are loosely bonded and can be easily destroyed by electrostatic repulsion. This observation challenges the previous classification (7), which considers 100−200 nm ND aggregates as strongly bonded core aggregates.

The pH stability range for the NaCl milled ND (Figure 2c) is larger and the isoelectric point is achieved in a more acidic environment as compared to the sucrose milled ND (Figure 2d). This can result from different changes in the surface chemistry of ND caused by the two different milling media. In particular, ionic NaCl crystals could promote the formation of a dissociable surface species, while molecular solids, such as sucrose, do not. This hypothesis was investigated via FTIR spectroscopy (Figure 4). The spectra show that sucrose milled ND has more pronounced OH peaks (stretching at ~3430 cm^{-1} and bending at 1640 cm^{-1} (22)) when compared to NaCl milled ND. Furthermore, the ratio of C═O stretching at ~1730 cm^{-1} to the OH bend is higher for NaCl milled ND, which is indicative of more COOH rather than OH groups on the surface of ND after milling with NaCl. Still, further mechanochemistry studies are needed to understand details of this effect since it could reveal the means for possible functionalization of ND in the process of its deaggregation.

ND samples milled for 90 min with NaCl or sucrose after pH adjustment both form stable dark translucent colloidal solutions with particle diameter maxima at 16−18 nm

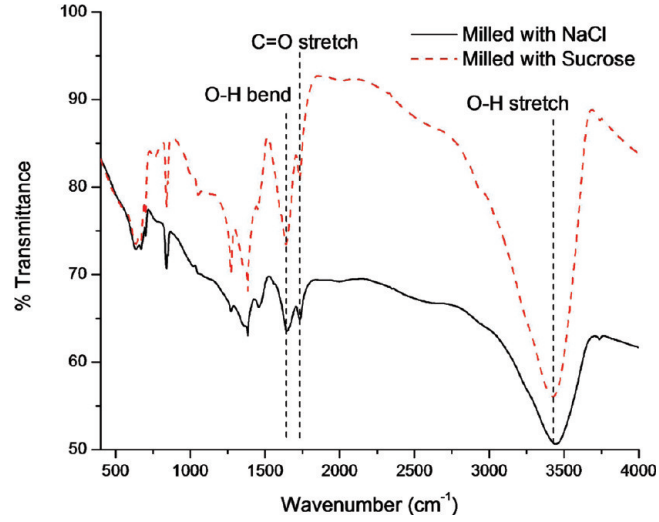

FIGURE 4. FTIR spectra recorded for NaCl- and sucrose-milled ND powders immediately after milling, before any rinsing.

(Figure 1c, d). The dark translucent appearance of colloidal solutions is typical for single digit ND particles (15, 16), suggesting that large aggregates that scatter light were eliminated in this milling regime. The dark color of single digit ND colloidal solutions is not yet explained. However, it is sometimes hypothesized to originate from graphitic or amorphous sp^2 carbon on the surface of ND (see, for example, ref 16). Analysis of our milled pH adjusted samples rules out the latter hypothesis. The small amounts of 0.1 M NaOH we used to shift the pH of the milled ND suspensions cannot induce the conversion of diamond into graphitic or amorphous carbon; nevertheless, the suspension turns from opaque pale brown into translucent dark brown in a matter of seconds upon adding the base (see inset in Figure 2c). Thus, we conclude that the dark brown color of aqueous ND

colloidal solutions is not because of graphitic or amorphous carbon. This optical characteristic of ND colloidal solutions still needs to be further studied.

An increase in milling time up to 5 h with subsequent pH adjustment results in a further reduction in particle size and an increase of proportion of smaller ND aggregates with subten-nanometer diameter particles eventually dominating the PSD in the case of NaCl milled pH adjusted colloidal solution (Figure 2a). This corresponds to 1−2 primary particles given that the diameter of a ND particle is ∼5 nm. However, in our experiments we never observed PSD of colloidal ND solutions peaks at 5 nm, which is commonly considered as an indicative of single digit diamond suspension. There could be several reasons why there is no 5 nm particles peak in PSD even after 5 h milling. First, the PSD can be affected by a fraction of larger primary ND particles present in our ND sample (23). It has been shown before (24) that the nanodiamond we used in this study contains a fraction of 15−30 nm primary particles which can be detected by TEM, XRD, and Raman spectroscopy after burning off smaller ND particles in air. The presence of the larger primary particles may result in a shift toward larger sizes in the PSD of the milled samples. Second, the ND aggregates observed after milling could be dynamic in nature, that is, on one hand, continuously formed because of collisions between few ND primary particles and held together by the weak interparticle interactions; on the other hand, continuously destroyed due to collisions with other particles and with molecules of the environment. Thus, there is a dynamic equilibrium between the ND aggregates and primary particles in colloidal solution, similar to that observed for chemical reactions (eq 2):

$$(\mathrm{ND})_n \leftrightarrow n\mathrm{ND} \qquad (2)$$

An argument in favor of the dynamic aggregates hypothesis is a large scatter often observed between PSD curves recorded repeatedly (10−20 times) for the same sample.

Finally, it is important to note that the milled ND material produced in this study could be dried and redispersed again producing suspensions with same small particles. To verify this, both pH adjusted solutions of NaCl- and sugar-milled ND were dried and redispersed in DI water. The measured PSD curves presented in Figure 1c and d show that the results remain consistent, with a peak at 16−18 nm.

4. CONCLUSIONS

Dry media assisted milling was demonstrated as a novel, simple, inexpensive, and efficient alternative to the current ways of deaggregation of nanodiamond. The technique uses water-soluble nontoxic and noncontaminating crystalline compounds such as sodium chloride or sucrose. When milling is complete, the media can be easily removed from the product by simple water rinsing, which provides a remarkable advantage compared to milling with any kind of ceramic microbeads. Using the dry media assisted milling with subsequent pH adjustment, it is possible to produce stable aqueous nanodiamond colloidal solutions with particles <10 nm in diameter, which corresponds to 1−2 primary ND particles. The study of milling kinetics and characterization of the produced ND colloids led us to conclude that small aggregates <200 nm in diameter, observed at the tail of the PSD of milled nanodiamond, are loosely bonded and rather dynamic in nature, thus challenging the hypothesis of the insurmountable bond strength of ND core aggregates. Color change observed in ND colloids upon shifting their pH toward the basic end allowed us to demonstrate that the coloration comes from the light interaction with colloidal particles, thus ruling out the previous hypothesis ascribing the dark color of single digit ND solutions to amorphous and graphitic carbon impurities.

Acknowledgment. We thank NanoBlox, Inc., U.S.A. for providing ND powder. We are grateful to the Centralized Research Facility (CRF) of the College of Engineering for providing access to the TEM. A.P. was supported by Drexel University's Research Co-op program, and V.M. and Y.G. were supported by an NSF grant CMMI-0927963.

REFERENCES AND NOTES

(1) Danilenko, V. V. *Solid State Phys.* **2004**, *46*, 595–9.
(2) Greiner, N. R.; Phillips, D. S.; Johnson, J. D.; Volk, F. *Nature* **1988**, *333*, 440–2.
(3) Shenderova, O. A.; Gruen, D. M. Ultrananocrystalline diamond: synthesis, properties, and applications. William Andrew Pub.: Norwich, N. Y., 2006.
(4) Liamkin, A. I.; Petrov, E. A.; Ershov, A. P.; Sakovich, G. V.; Staver, A. M.; Titov, V. M. *Dokl. Akad. Nauk SSSR* **1988**, *302*, 611–3.
(5) Ho, D., Ed. Nanodiamonds: Applications in biology and nanoscale medicine. Springer: New York, 2010.
(6) Osawa, E. D. Ho, Ed. Nanodiamonds: Applications in biology and nanoscale medicine. Springer: New York, 2010; pp 1−33.
(7) Kruger, A.; Kataoka, F.; Ozawa, M.; Fujino, T.; Suzuki, Y.; Aleksenskii, A. E.; Vul, A. Y.; Osawa, E. *Carbon* **2005**, *43*, 1722–1730.
(8) Barnard, A. S. *J. Mater. Chem.* **2008**, *18*, 4038–4041.
(9) Barnard, A. S.; Stenberg, M. *J. Mater. Chem.* **2007**, *17*, 4811–9.
(10) Pichot, V.; Comet, M.; Fousson, E.; Baras, C.; Senger, A.; Le Normand, F.; Spitzer, D. *Diamond Relat. Mater.* **2008**, *17*, 13–22.
(11) Osswald, S.; Yushin, G.; Mochalin, V.; Kucheyuv, S. O.; Gogotsi, Y. *J. Am. Chem. Soc.* **2006**, *128*, 11635–11642.
(12) Xu, K.; Xue, Q. *Solid State Phys.* **2004**, *46*, 633–4.
(13) Xu, X. Y.; Yu, Z. M.; Zhu, Y. W.; Wang, B. C. *J. Solid State Chem.* **2005**, *178*, 688–693.
(14) Vul, A. Y.; Dideikin, A. T.; Tsareva, Z. G.; Korytov, M. N.; Brunkov, P. N.; Zhukov, B. G.; Rozov, S. I. *Tech. Phys. Lett.* **2006**, *32*, 561–3.
(15) Ozawa, M.; Inaguma, M.; Takahashi, M.; Kataoka, F.; Kruger, A.; Osawa, E. *Adv. Mater.* **2007**, *19*, 1201–6.
(16) Osawa, E. *Diamond Relat. Mater.* **2007**, *16*, 2018–2022.
(17) Xu, X. Y.; Zhu, Y. W.; Wang, B. C.; Yu, Z. M.; Xie, S. Z. *J. Mater. Sci. Technol.* **2005**, *21*, 109–112.
(18) Xu, Y. Y.; Yu, Z. M.; Zhu, Y. M.; Wang, B. C. *Diamond Relat. Mater.* **2005**, *14*, 206–212.
(19) Mochalin, V. N.; Sagar, A.; Gour, S.; Gogotsi, Y. *Pharm. Res.* **2009**, *26*, 1365–1370.
(20) Schilling, R. *Ceram. Ind.* **2008**, 12–5.
(21) Tu, J. S.; Perevedentseva, E.; Chung, P. H.; Cheng, C. L. *J. Chem. Phys.* **2006**, 125.
(22) Mochalin, V.; Osswald, S.; Gogotsi, Y. *Chem. Mater.* **2009**, *21*, 273–9.
(23) Osswald, S.; Mochalin, V. N.; Havel, M.; Yushin, G.; Gogotsi, Y. *Phys. Rev. B: Condens. Matter Mater. Phys.* **2009**, 80.
(24) Osswald, S.; Havel, M.; Mochalin, V.; Yushin, G.; Gogotsi, Y. *Diamond Relat. Mater.* **2008**, *17*, 1122–6.

AM100720N